J Nanopart Res (2019) 21: 64
https://doi.org/10.1007/s11051-019-4499-0

RESEARCH PAPER

Effect of PAA-coated magnetic nanoparticles on the performance of PVA-based hydrogels developed to be used as environmental remediation devices

Laura M. Sanchez · Daniel G. Actis · Jimena S. Gonzalez · Pedro Mendoza Zélis · Vera A. Alvarez

Received: 15 June 2018 / Accepted: 6 March 2019 / Published online: 22 March 2019

Abstract In the present work, the effect of the incorporation of polyacrylic acid (PAA)–coated magnetic nanoparticles (MNPs) on the performance of polyvinyl alcohol (PVA)–based hydrogels for water remediation was studied. Ferrogels from PVA and PAA-coated MNPs were prepared through the ecocompatible freezing–thawing physical cross-linking method, and then they were completely characterized. Two different lab-made PAA-coated iron oxide MNPs, characterized in a previous work, were prepared by coprecipitation method from two different low PAA molecular weights, Mw 1800 g/mol and 5000 g/mol. The effect of MNP content and the PAA Mw on ferrogel final properties was determined. In addition, adsorption of methylene blue (MB) and cadmium (Cd^{+2}) was carried out to analyze the possible application of the developed materials as environmental remediation devices. The capture of a ferrogel by an external field occurs due to the force that the field gradient exerts on single magnetic particles, which is then transferred onto the polymer matrix. This force was measured as a function of the distance to a permanent magnet, and the condition to magnetically recover the sample was established. The results obtained demonstrated that the ferrogels presented in this work are able to adsorb heavy metals and then be magnetically separated.

Keywords Magnetic hydrogel · Ferrogel · Iron oxide nanoparticles · Nanocomposite · Polyvinyl alcohol · Polyacrylic acid · Environmental remediation

L. M. Sanchez (✉) · J. S. Gonzalez · V. A. Alvarez
Materiales Compuestos Termoplásticos (CoMP), Instituto de Investigaciones en Ciencia y Tecnología de Materiales (INTEMA), CONICET - Universidad Nacional de Mar del Plata (UNMdP), Av. Colón 10890, 7600 Mar del Plata, Argentina
e-mail: lsanchez@mdp.edu.ar

D. G. Actis · P. M. Zélis
Instituto de Física de La Plata (IFLP), CONICET-Departamento de Física, Universidad Nacional de La Plata (UNLP), 1900 La Plata, Argentina

Introduction

Hydrogels are three-dimensional networks formed by permanent (chemical) or reversible (physical) unions whose more outstanding characteristic is related to their large swelling properties (Ahmed 2015). Polyvinyl alcohol (PVA) is widely used for hydrogel preparation due to its hydrophilic, relatively inert, and ease-to process characteristics (Peppas and Tennenhouse 2004). PVA hydrogels have been prepared by chemical cross-linking methods by employing chemical agents such as glutaraldehyde and formaldehyde, and also by physical ones through the formation of crystallites by freezing–thawing cycles (F-T) and by annealing using heating and cooling (Peppas and Tennenhouse 2004; Gonzalez and Alvarez 2011). The advantages offered on employment of physical cross-linking methods are related to obtained environmental-friendly and low-toxicity hydrogels.

The employment of stimuli-responsive starting materials for hydrogels preparation has opened a broad set of applications, including biomedical and

environmental fields. External stimuli such as pH, electrical and/or magnetic fields, ion strength, temperature, and light, among many other ones, could change the hydrogel swelling and adsorption behaviors, permeability, and elasticity in a reversible manner (Mansur et al. 2008; Bardajee et al. 2013; Majid et al. 2015; Sanchez et al. 2017). Furthermore, small amounts of inorganic nanometric fillers are usually added to improve hydrogel mechanical properties, thermal stability, electrical, optical, permeability, and chemical properties. Among the most employed inorganic fillers, clays, metal oxides, carbon, and metals could be mentioned (Sinha Ray and Okamoto 2003; Sun et al. 2004; Sanchez et al. 2018b).

Magnetic hydrogels, usually called ferrogels, are stimuli-responsive, as their motion can be controlled by an external magnetic field. This provides ferrogels unique properties: they can be used to adsorb heavy metals and then be magnetically separated. The capture of a ferrogel by an external field occurs due to the force that the field gradient exerts on single magnetic particles, which is then transferred onto the polymer matrix.

In a field gradient, the magnetic particles tend to move to the region with a higher field. Therefore, if the magnetic field is generated through a permanent magnet, the magnetic force tends to move the ferrogel to the magnet. If the intensity of the magnetic force is enough to get over the gravitational force, the sample will move to the magnet until be attached.

Ferrogels were prepared in diverse compositions from different inorganic fillers and matrices in accordance with the desired application (Timko et al. 2010; Kim et al. 2012; Bardajee et al. 2013; Reddy and Lee 2013; Sanchez et al. 2017; Sekhavat Pour and Ghaemy 2015; Sun et al. 2015). The use of PVA and magnetite as starting materials for obtaining ferrogels and their corresponding characterization have been reported (Goiti et al. 2007; Timko et al. 2010; Mendoza Zelis et al. 2013; Gonzalez et al. 2014). Magnetic and structural properties of some PVA ferrogels containing commercial polyacrylic acid (PAA)-coated iron oxides have been studied (Mendoza Zelis et al. 2013; Moscoso-Londono et al. 2013; Sanchez et al. 2016). PAA is a hydrophilic, biocompatible polymer having a polyanionic structure whose pKa is found between 4.5 and 5.0 (Manavi-Tehrani et al. 2010; Majid et al. 2015).

The lack of good-quality hydric resources, mostly associated with their pollution due to industrial and agrochemical activities, is a worldwide problem. Dyes are very stable towards oxidizing agents, humidity, solar radiation, and microbial attacks (Nigam et al. 2000; Kumar and Tamilarasan 2013; Sanchez et al. 2016), and their potential mutagenic and carcinogenic effects have been reported. Furthermore, intrinsic persistence and toxicity of heavy metals present in soils and aqueous environments are problems too (Alghanmi et al. 2015). Since human life is strongly dependent to both water consumed and industrialized products, it is necessary to achieve not only the remediation of the affected resources, but also the production of materials (those already known and also new-ones) through alternative ways capable to minimize the negative environmental effects.

In the present work, we prepare and characterize ferrogels from PVA and PAA-coated magnetic nanoparticles (MNPs) through the ecocompatible F-T physical cross-linking method. Two different lab-made PAA-coated iron oxide MNPs were prepared by coprecipitation method from two different low PAA molecular weights, Mw 1800 g/mol and 5000 g/mol. The effect of MNP content and the PAA Mw on ferrogel final properties was exhaustively studied. In addition, adsorption of methylene blue (MB) and cadmium (Cd^{+2}) was carried out to analyze the possible application of the developed materials as environmental remediation devices. Finally, the magnetic force generated for a permanent magnet on the ferrogels was measured to determine if it is possible to magnetically capture the ferrogels after water treatments.

Materials and methods

Materials

PVA was supplied by Sigma-Aldrich (molecular weight 89,000–98,000 g/mol, hydrolysis degree of 98–99%). For iron oxide MNP preparation, two different iron salts were used as starting materials: $FeSO_4.7H_2O$ and $FeCl_3.6H_2O$ (both from Cicarelli Laboratory, Argentina). Furthermore, two PAA were employed: Mw 1800 g/mol and 5000 g/mol both purchased from Polysciences. Other reactants were also incorporated: NH_4OH (Biopack, Argentina) and bidistilled water.

Methylene blue (MB) and cadmium (Cd^{+2}) were used as model pollutants to perform adsorption tests.

Preparation and characterization of hydrogels

The hydrogels prepared from PVA and iron oxide MNPs were synthesized according to our previously reported

technique (Gonzalez et al. 2016). First, two different PAA-coated iron oxide MNPs were prepared by coprecipitation method from two different low PAA molecular weights, Mw 1800 g/mol and 5000 g/mol. Then, they were characterized by X-ray diffraction (XRD), thermogravimetric analysis (TGA), Fourier transformed infrared spectroscopy (FTIR), transmission electron microscopy (TEM), Z-potential, dynamic light scattering (DLS), and magnetic measurements. A detailed description of these materials was previously published by our research group (Sanchez et al. 2018a). Then, a 10 *w/v*% PVA water solution was prepared, and different amounts of the MNPs were incorporated to this to perform a series of ferrogels. The suspensions were maintained under constant stirring (with a magnetic bar) at 85 °C during 4 h. After this, the composites were cast onto a series of anti-adherent containers. The physically cross-linked hydrogels through the freezing–thawing (F-T) cycles method were obtained by frozen (− 18 °C, 1 h) and then placed at room temperature (25 °C, 1 h), completing three of F-T cycles. PVA and PVA/PAA hydrogel control samples were obtained by following the same general procedure, but without the addition of the MNPs. A schematic procedure is presented in Fig. 1.

A complete characterization of the different hydrogels was conducted. Measurements of dried samples have been carried out by XRD in an analytical expert instrument for 2θ values from 10 to 65 degrees at a rate of 2°/min. For this, monochromatic Cu-Kα radiation was employed. TGA was conducted in a TA-Q500 equipment at room temperature of 900 °C under air atmosphere at a heating rate of 10 °C/min. FTIR measurements were done in a Thermo Scientific Nicolet 6700 spectrometer, employing a resolution of 4 cm^{-1}. Measurements were carried out in attenuated total reflectance modes (smart Orbit ATR accessory) from 400 to 4000 cm^{-1}. The morphology of hydrogels was analyzed from Field Emission Scanning Electron micrographs (FESEM) in FESEM Zeiss Supra equipment and scanning electron micrographs (SEM) and in a JEOL JSM-6460 LV instrument. Samples have been previously swollen, frozen, lyophilized, cryofractured with N_2 liquid, and sputtered with gold. At least 200 measurements had been averaged. Swelling degree measurements and gel fraction determinations (GF%) were carried out in buffer solutions and in distilled water both at 25 °C, respectively. The equilibrium swelling degree (M_∞%) was determined by the following equation (Eq. 1):

$$M_\infty(\%) = \frac{W_f - W_i}{W_i} \times 100 \quad (1)$$

where W_i is the weight of the samples before immersion and W_f is the weight of the sample at equilibrium water content.

To perform GF% measurements, a slice of each sample was immersed into distilled water at room temperature during 4 days to rinse away unreacted species. Then, the sample was removed from distilled water and dried at 37 °C until constant weight was reached. Therefore, the gel fraction can be calculated as follows (Eq. 2):

$$GF(\%) = \frac{W_f - W_r}{W_i - W_r} \times 100 \quad (2)$$

where W_i and W_f are the weights of the dried hydrogels before and after immersion, respectively, and W_r is the weight of the filler added (experimentally determined by TGA).

Furthermore, the magnetic properties (saturation magnetization and susceptibility) were studied in a Lakeshore 7404 vibrating sample magnetometer (VSM).

The crystallinity degree of model prepared samples was obtained from differential scanning calorimetric (DSC) measurements, which were carried out in a Shimadzu DSC-50 at room temperature of 255 °C at 10 °C/min, under N_2 atmosphere. For this, hydrogel samples were previously dried for 48 h at 40 °C. The crystallinity degree (X_{cr}%) was calculated from the following equation:

$$X_{cr}(\%) = \frac{\Delta H}{\Delta H^\circ \times W_{PVA}} \times 100 \quad (3)$$

where ΔH was determined by integrating the area under the melting peak and ΔH° is the heat (138.6 J/g) required for melting a 100% crystalline PVA sample, whereas W_{PVA} is the mass fraction of the PVA matrix in the hydrogel sample.

Dye adsorption measurements

The different assays conducted to determine the capability of the selected nanocomposite towards MB and cadmium (Cd^{+2}) adsorption were carried out on separated batch aqueous solutions of each model pollutant. The MB solution was 10 mg/L, whereas the Cd^{+2} solution concentration was 100 mg/L. Adsorption was achieved by adding a known amount of adsorbent into

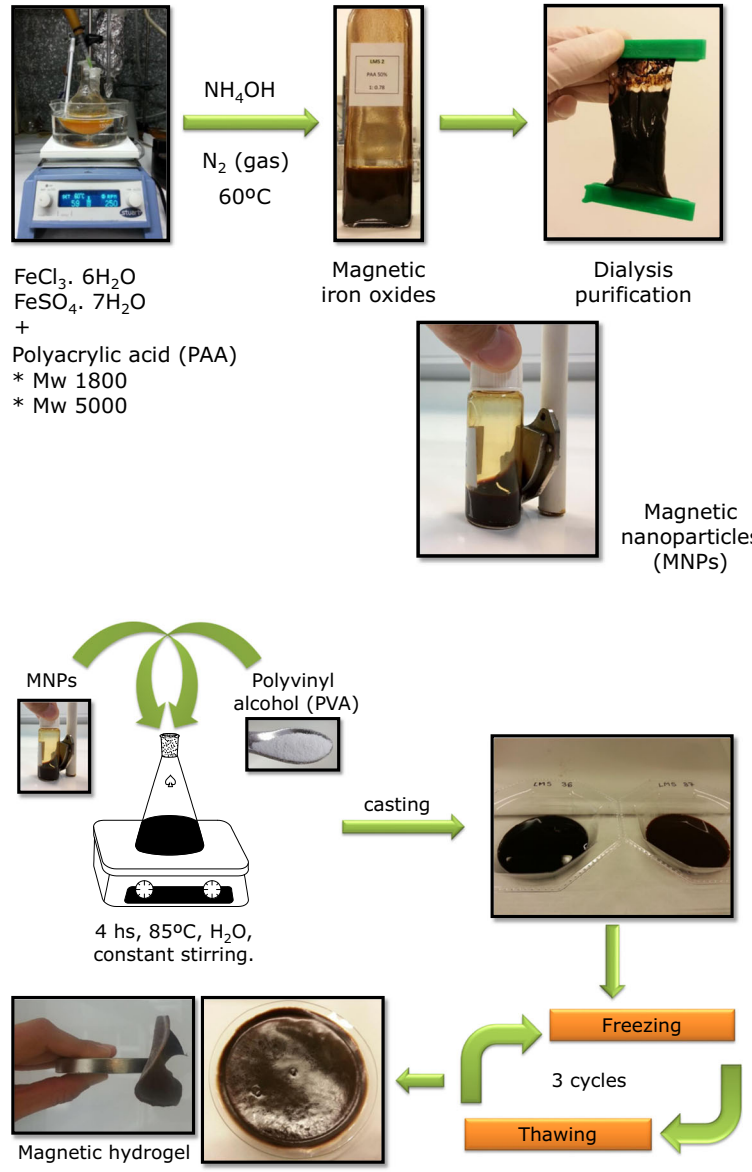

Fig. 1 Ferrogel preparation schematic procedure

a specific volume of dye solution of known concentration. In the case of MB removal, the progress of each treatment was monitored by using a UV–visible spectrometer. The spectra were acquired with a SQ-2800E UNICO diode array spectrophotometer, in the range from 300 to 900 nm, paying special attention to λ_{max} = 664 nm. Different tests were conducted with and without the application of an external magnetic field (300 mT during all treatment).

For Cd^{+2} adsorption tests, measurements were conducted by atomic absorption spectroscopy using a GBC Avanta 932 equipment. Blank experiments were performed by employing the PVA hydrogel. Results are expressed as removal efficiency at t time R_t (%) (Eq. 4):

$$R_t(\%) = \frac{C_0 - C_t}{C_0} \times 100 \quad (4)$$

where C_0 (mg/L) refers to the initial concentration of the pollutant and C_t (mg/L) corresponds to the remaining concentration at t time. Adsorbed amount at t time q_t (Eq. 5) was also employed to present the results:

$$q_t = (C_0 - C_t) \times \frac{V}{W} \quad (5)$$

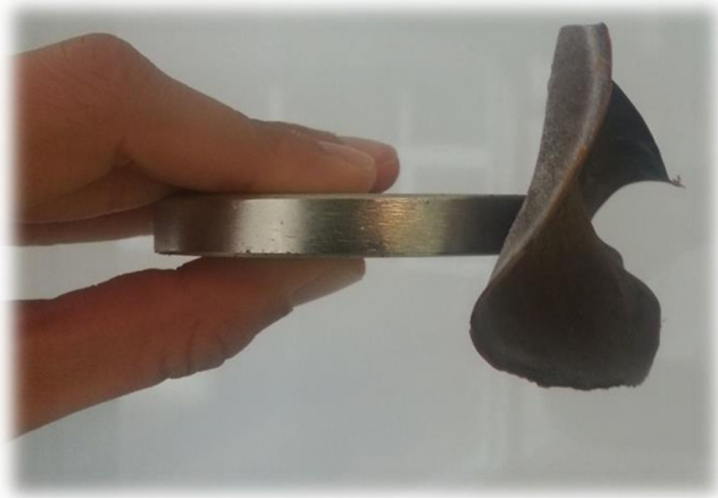

Fig. 2 Ferrogel response under the presence of a permanent magnet

where C_0 (mg/L) refers to the initial concentration of the selected model pollutant, C_t (mg/L) corresponds to the remaining concentration at t time, V is the MB/Cd^{+2} solution volume used (L), and W is the employed sorbent mass (mg).

Magnetic force measurements

The ferrogels' magnetic response was also analyzed from the point of view of the magnetic force, as this magnitude reflects the viability of the ferrogels' recovery after the adsorption has occurred. Each sample was put on a nonmagnetic base on a RADWAG PS 1000/C/2 balance. A cylindrical $Nd_2Fe_{14}B$ magnet of 5 cm diameter and 1.2 cm height rested on a platform of variable height, aligned with the sample. In this way, the platform's vertical movement controls the magnet-sample distance, while the balance's weight lecture decreases with the magnetic force. The sample was held in place by a small, nonmagnetic weight, otherwise, it would have been lifted once the magnetic force exceeded the sample weight. The minimum height of the magnet surface above the sample was of 12 ± 1 mm.

The magnet-sample distance determines the field $\overrightarrow{H}$ applied to the sample, which in turn magnetizes the ferrogel. The resulting vertical component of the magnetic force (F_z) per unit weight (mg) is the product of the mass magnetization (M_z) and the gradient of the magnetic field $\left(\frac{\partial H_z}{\partial z}\right)$ divided the gravitational acceleration (g). Both the field and its gradient are functions of the magnet-sample distance (z).

$$\frac{F_z}{\mathrm{mg}} = \frac{\mu_0 M_z}{g}\frac{\partial H_z}{\partial z} \tag{6}$$

where μ_0 is the vacuum permeability.

Table 1 Some of the most relevant characteristics of developed ferrogels

PAA Mw = 1800				PAA Mw = 5000			
MNPs (%)	GF (%)	PAA (%)	Tp (°C)	MNPs (%)	GF (%)	PAA (%)	Tp (°C)
0	88.0 ± 0.8	0.00	284	0	88.0 ± 0.8	0.00	284
2.2	86.3 ± 1.0	1.21	312	2.3	86.2 ± 2.4	1.28	316
3.4	83.6 ± 1.3	1.96	303	4.8	84.8 ± 2.2	3.69	307
5.8	81.6 ± 1.7	3.17	293	5.5	77.9 ± 3.1	4.21	305
7.8	75.0 ± 0.7	4.29	292	8.4	73.1 ± 0.8	7.35	296
10.1	67.0 ± 1.7	5.90	297	11.2	70.1 ± 2.7	8.61	289

Results and discussion

Preparation and characterization of PVA/MNP hydrogel

Magnetically responsive nanocomposite hydrogels based on PVA and different concentrations of two different MNPs prepared by the F-T technique which is an economic, non-hazardous, and facile method were effectively obtained (Fig. 2).

Regarding MNPs characterization, the iron oxide content (60 wt.%) was determined by TGA, while its nature was analyzed by XRD: they consist in an iron oxides mixture, mainly composed by magnetite. Crystallite sizes were approximately 9 nm for MNPs prepared with PAA's Mw 5000 and 11–13 nm for those prepared employing PAA's Mw 5000. Magnetization results revealed the preparation of superparamagnetic MNPs. For a complete understanding of these systems, our previous paper could be consulted (Sanchez et al. 2018a).

The prepared MNPs were used as a filler of PVA hydrogels in different proportions. After subtraction of carbonaceous residues arising from incomplete degradation of PVA (1 wt%) and bound water, the MNP content was determined by TGA. From TGA results of the characterized MNPs, and the corresponding TGA measurements obtained for each ferrogel, the PAA content in each composite hydrogel was inferred. Some of the most relevant characteristics of ferrogel systems are summarized in Table 1.

From the previous table, it is possible to observe that the GF, which is an indicator parameter of the cross-linking degree of hydrogels, depends on both, the particle content and the PAA contents. It is important to note that, independently of the Mw of the PAA, GF clearly decreased as a function of both, MNP and PAA contents. Regarding nanoparticles, some authors have shown that the incorporation of a small amount of properly functionalized magnetic nanoparticles within hydrogel matrices causes the opening of the polymer network, acting as cross-linking knots that make possible the formation of a more porous structure and with a great hydration capacity (Bonhome Espinosa 2017).

On the other hand, it can be observed that the degradation temperature (Tp, Table 1) was higher for ferrogels (round near and also greater than 300 °C) than for hydrogels (285 °C). This phenomenon is possibly associated with a strong interaction between the matrix and the nanometric phase. These polymer–MNP interactions restrict the mobility of the polymer chains thus reducing the diffusion of heat within the matrix, so the MNPs act as a thermal barrier delaying the degradation of the matrix (Goiti et al. 2007). It can also be observed that the Tp increase is independent of the molecular weight of the PAA used.

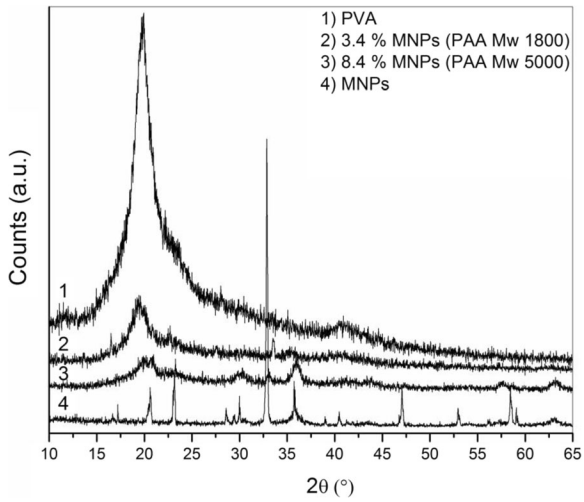

Fig. 3 XRD spectra for PVA matrix, MNPs, and ferrogels with different contents of MNPs coated with PAA of different molecular weights

In order to conduct a qualitative study of the prepared materials, XRD measurements were performed for the PVA matrix, MNPs and both kind of ferrogels with different MNPs contents (Fig. 3).

The main characteristic diffraction peaks of semi-crystalline PVA located at 19.8° and 22.9° (2θ) which correspond to the (1 0 1) and (1 0 1) reflection planes, respectively, are present in the PVA and also in the

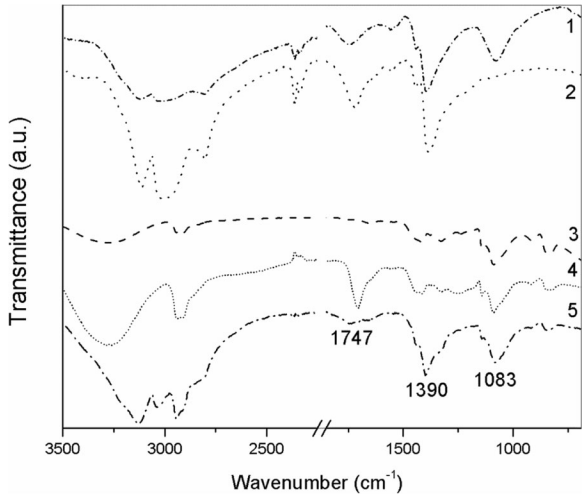

Fig. 4 FTIR spectra of MNPs (1), PAA (2), PVA (3), PVA/PAA (4), and ferrogel PVA/MNPs 5.8% (5)

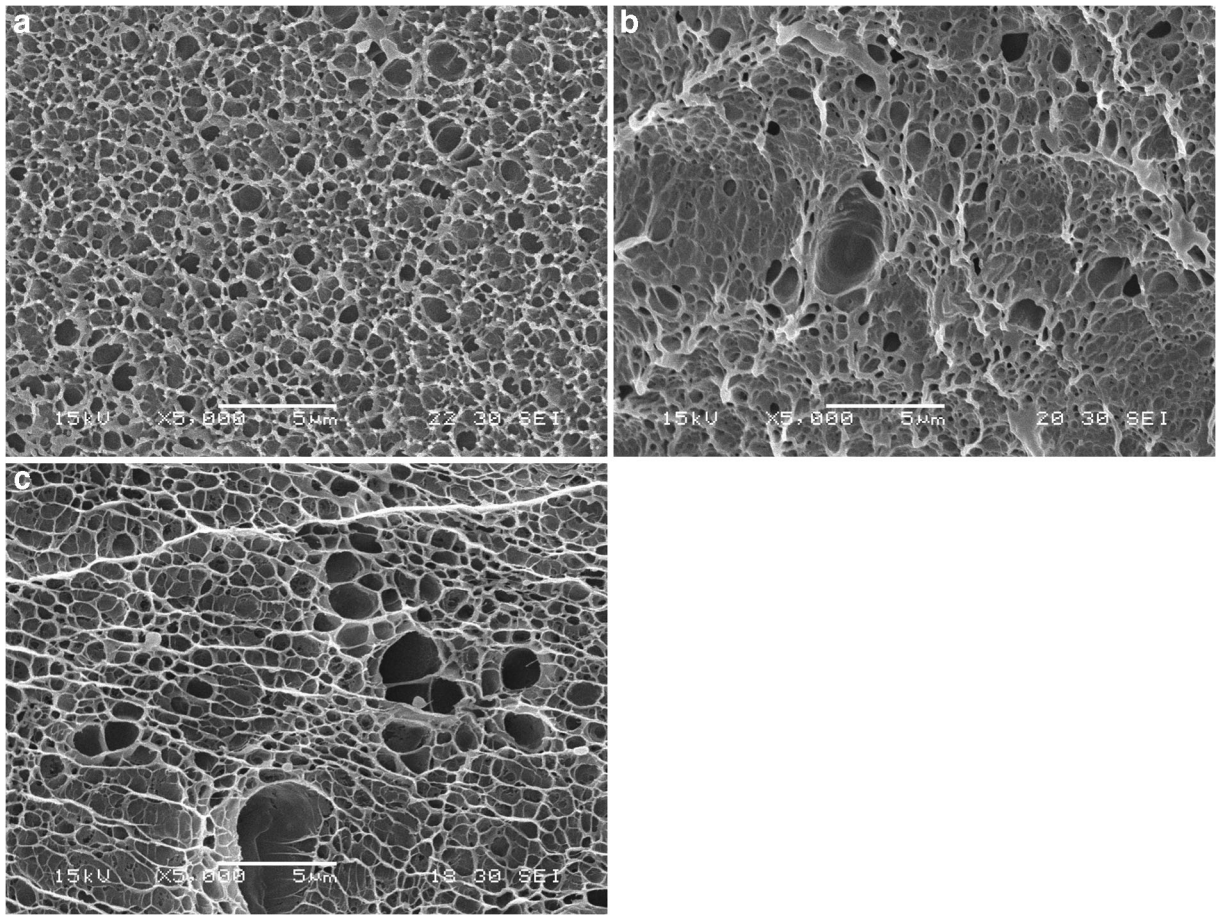

Fig. 5 SEM images (magnification × 5000) of PVA hydrogel (**a**) and ferrogels with around 2 wt.% of MNPs coated with PAA of different Mw 1800 (**b**) and 5000 (**c**)

ferrogels diffractograms (Ricciardi et al. 2004; Gupta et al. 2009). In the case of ferrogels, very intense peak centered at 35.5° (2θ) was observed. This peak agrees with the (3 1 1) plane reflection, the most intense diffraction peak for

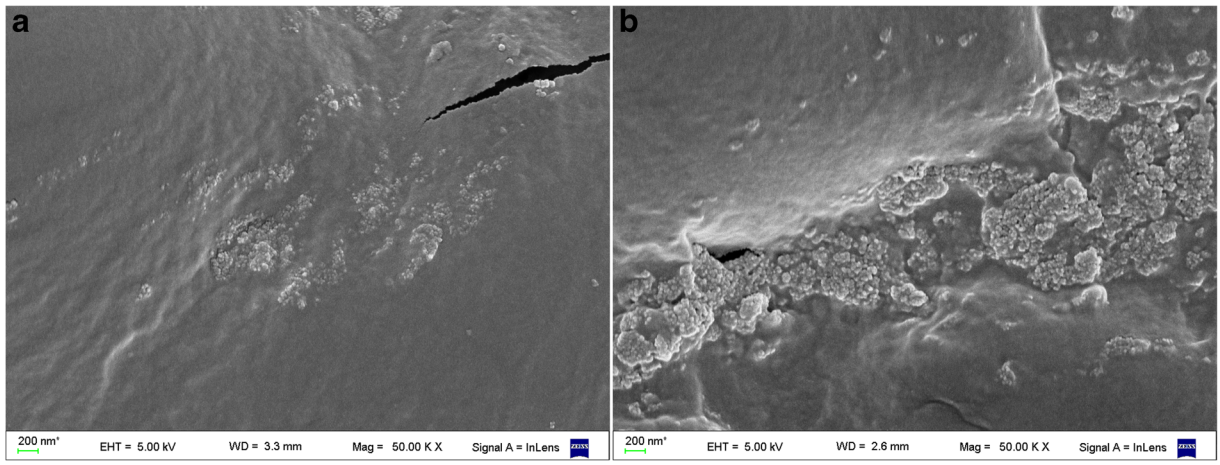

Fig. 6 FESEM images of ferrogels containing around 2 wt.% of MNPs coated with PAA of different Mw 1800 (**a**) and 5000 (**b**) (magnification × 50,000)

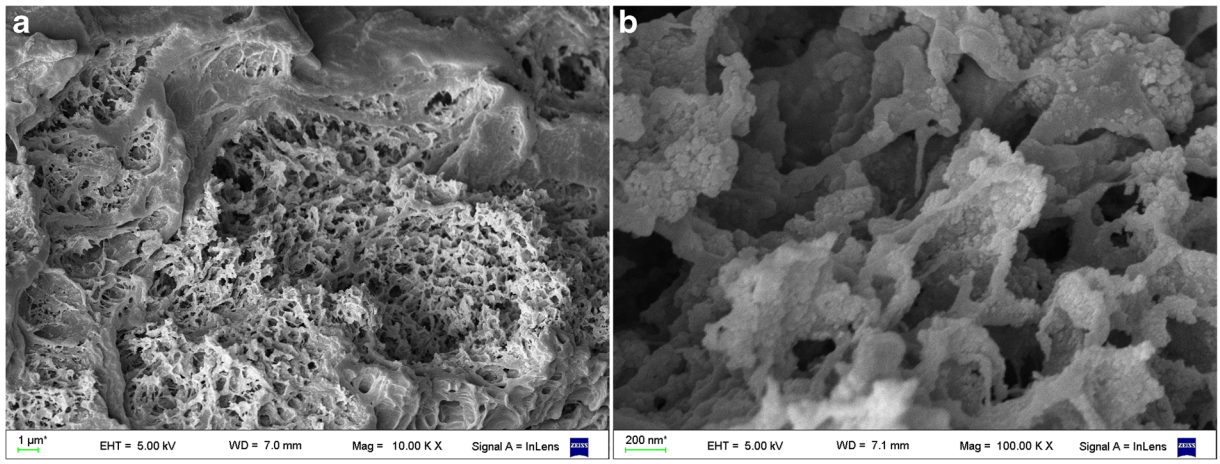

Fig. 7 FESEM images of a ferrogel containing around 8.4 wt.% of MNPs coated with PAA of Mw5000 (magnification × 10,000 (**a**) and × 100,000 (**b**))

magnetite (*19–0629 JCPDS, Joint Committee on Powder Diffraction Standards*) and confirms the presence of this iron oxide in the PVA matrix. Other minor diffraction peaks corresponding to the iron oxides coated by PAA are present in the ferrogels samples, such as those located at $2\theta = 20°$, 30.2°, 32.8°, 43.4°, 53.7°, 57.4°, and 62.9° (Lin et al. 2005; Sanchez et al. 2018a).

For comparison purposes, Fig. 4 shows the FTIR spectra of PVA matrix, PAA, PVA-PAA hydrogel, MNPs, and a representative ferrogel. PVA spectrum presents its typical expected band centered at 3288 cm^{-1} corresponding to the O–H stretching vibration (Manavi-Tehrani et al. 2010), whereas ferrogel spectra not only do not present free OH bands (3650–3600 cm^{-1}) but also have hints of hydrogen bonding existence (3570–3200 cm^{-1}) (Mansur et al. 2004; Chen and Zhang 2010). Then, the C=O band is present at 1718 cm^{-1}as expected for the PAA and PVA/PAA samples, it is absent in the PVA and it is shifted to 1747 cm^{-1} for the ferrogel. While it could be though that the ester C=O band would correspond to an ester linkage between PVA and PAA, in this physically crosslinked systems the 1747 cm^{-1} band corresponds to ester linkages between PAA and the iron oxides in the MNPs (Sanchez et al. 2018a). Furthermore, the 1390 cm^{-1} band present in ferrogels corresponds to the symmetrical –COO stretching and its position indicates than iron oxides surface and PAA functional groups are interacting (Sanchez et al. 2018a). Finally, the 1083 cm^{-1} band of the ferrogel could be attributed both to a crystalline effect of the PVA and to the symmetrical –COO stretching of PAA present in the MNPs, or a mixed contribution (Smith et al. 2009; Sanchez et al. 2018a).

The porous nature of the matrix and both kinds of ferrogels was confirmed by SEM analysis (Fig. 5).

Similar structures were observed for all studied gels. The presence of a homogeneous dispersion of small particles for ferrogels obtained from both kinds of MNPs was confirmed by FESEM (Fig. 6).

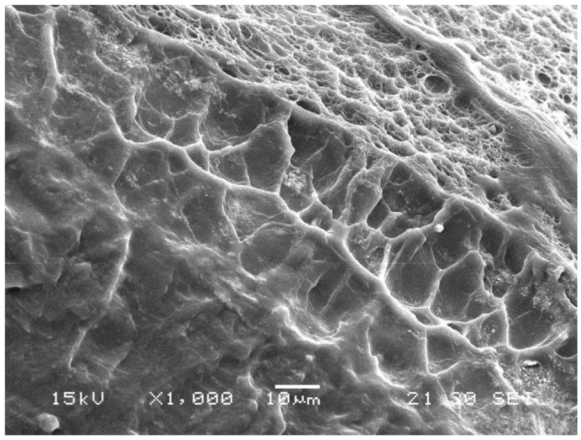

Fig. 8 SEM micrograph of a ferrogel containing around 8.4 wt.% of MNPs coated with PAA of Mw 5000 (magnification × 1000)

Table 2 Porous sizes of the prepared ferrogels (from SEM results)

PAA Mw = 1800		PAA Mw = 5000	
MNPs (%)	Porous size (µm)	MNPs (%)	Porous size (µm)
0	0.770 ± 0.260	0	0.770 ± 0.260
2.2	0.586 ± 0.268	2.3	0.283 ± 0.170
3.4	0.617 ± 0.263	4.8	0.795 ± 0.417

Table 3 Swelling of the developed ferrogels at different pH values

PAA Mw = 1800				PAA Mw = 5000			
MNPs (%)	M (%)		PAA (%)	MNPs (%)	M (%)		PAA (%)
	pH = 4	pH = 7			pH = 4	pH = 7	
0	191.6 ± 5.4	187.1 ± 16.0	0	0	191.6 ± 5.4	187.1 ± 16.0	0
2.2	154.3 ± 13.5	126.9 ± 1.5	1.21	2.3	183.7 ± 16.4	178.0 ± 10.6	1.28
3.4	172.1 ± 11.1	147.5 ± 3.1	1.96	4.8	208.7 ± 7.2	166.9 ± 4.1	3.69
5.8	200.1 ± 11.8	194.3 ± 3.3	3.17	5.5	185.8 ± 8.5	167.0 ± 4.1	4.21
7.8	190.7 ± 11.0	173.8 ± 8.2	4.29	8.4	152.3 ± 1.0	126.5 ± 1.8	7.35
10.1	222.1 ± 13.6	182.5 ± 6.6	5.90	11.2	170.9 ± 2.7	155.9 ± 0.6	8.61

Furthermore, homogeneous dispersion of MNPs was also obtained in ferrogels including high MNPs contents as can be seen in the following FESEM micrographs (Fig. 7):

Very outstandingly, it was possible to observe the presence of both pores and MNPs in a SEM micrograph of the ferrogel containing around 8.4 wt.% of MNPs coated with PAA of Mw 5000 (Fig. 8).

Regarding porous sizes, they were determined from SEM images through image processing by the employment of the Image Pro-Plus Software. For ferrogel samples, it was found an increment in the average size as a function of MNPs content (Table 2). Pores sizes are smaller or similar to those of neat PVA matrix.

Other important characteristic of hydrogels is related to their large swelling capacities that make them attractive not only as absorbents or separators but also as hosts for the development of multifunctional materials. The swelling of studied gels at different pH values is summarized in Table 3.

From Table 3, different tendencies can be observed for swelling. It is important to remember the factors that influence the swelling behavior. On one hand, the gel fraction has an important effect on swelling: the higher the GF, the lower the swelling degree (retaining all the other variables constant). On the other hand, the incorporation of a small amount of properly functionalized magnetic nanoparticles within hydrogel matrices causes the opening of the polymer network, acting as cross-linking knots that make possible the formation of a more porous structure and with a great hydration capacity (Bonhome Espinosa 2017). Finally, the functional groups employed as a coating of the MNPs (PAA) can also influence the observed behavior. Smart pH-responsive PVA-PAA blends for a variety of applications have been studied (Vazquez Torres et al. 1993; Byun et al. 2008; Sorber et al. 2008; Ray et al. 2009; Smith et al. 2009; Quintero et al. 2010). It is widely accepted that in this kind of materials the swelling capabilities rise when pH increases (Hickey and Peppas 1997; Peppas and Wright 1998; Peppas and Tennenhouse 2004). This fact is explained in terms of the ionization degree of –COOH groups present in PAA chains according to the pH in the medium. The repulsion interactions between $–COO^-$ produce an increase in the swelling of the network (Gudman and Peppas 1995; Quintero et al. 2010).

From DSC measurements ferrogels and matrix crystallinity degrees were determined according to Eq. 3. It was observed a X_{cr} decrease when MNPs content

Table 4 Magnetic properties of ferrogel samples: saturation magnetization (Ms) and susceptibility (χ)

PAA Mw = 1800				PAA Mw = 5000			
MNPs (%)	Ms (emu/g_{sample})	Ms (emu/$g_{iron\ oxides}$)	χ	MNPs (%)	Ms (emu/g_{sample})	Ms (emu/$g_{iron\ oxides}$)	χ
3.4	1.17	35.4	0.039	4.8	1.80	37.2	0.078
7.8	1.95	25.0	0.023	8.4	3.40	40.7	0.130
10.1	4.70	46.4	0.200	11.2	6.30	56.3	0.270

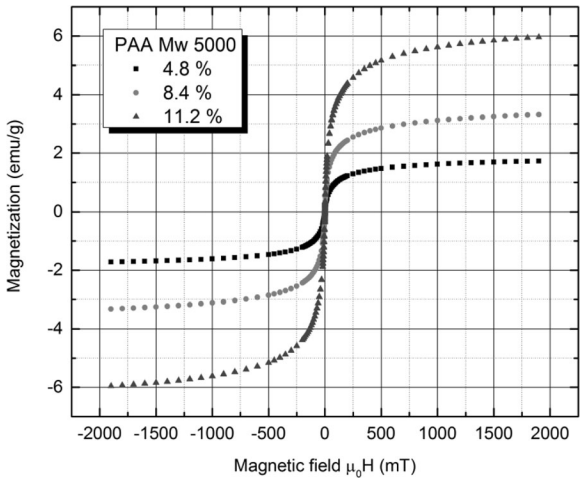

Fig. 9 Magnetization (in emu per gram of sample) vs. field curves for the PAA Mw = 5000 samples. Both saturation magnetization and susceptibility increase with MNP content

increases. For example, the ferrogel with 8.4% of MNPs (PAA Mw 5000) presented a X_{cr} of 13.5%, while X_{cr} for PVA matrix was found to be 24.8%. In this sense, the melting point was also found at a lower temperature for the 8.4% of MNPs (PAA Mw 5000) ferrogel (209.6°C) than for the neat PVA hydrogel (224.8°C). Those observations allow thinking that the presence of MNPs has an effect on both the crystal formation capability (less quantity than PVA matrix) and crystal size (smaller than

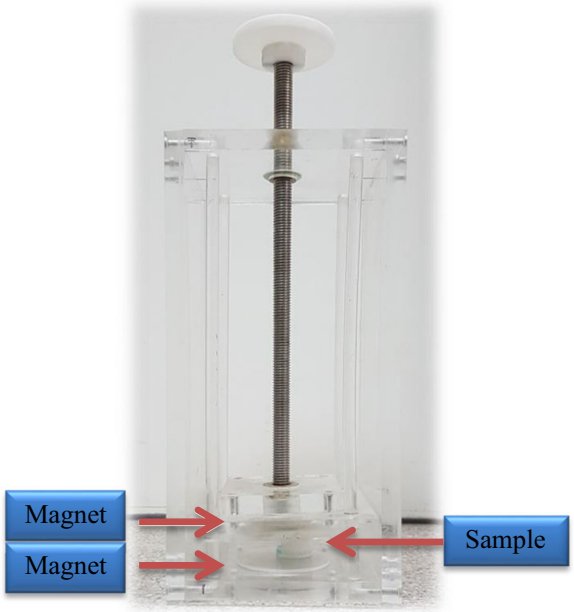

Fig. 10 Equipment designed to provide a specific external magnetic field during adsorption tests

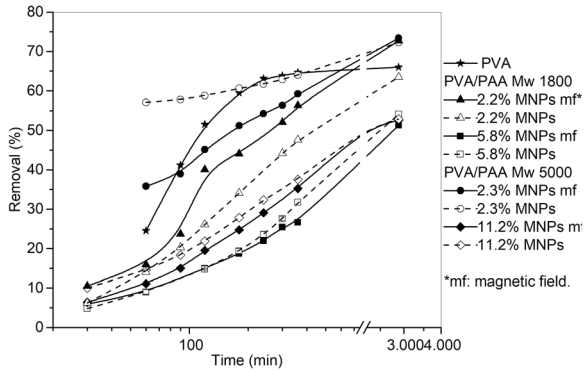

Fig. 11 Removal of MB by the PVA hydrogel and ferrogels with MNPs coated with PAA of different molecular weights, with and without magnetic field (mf)

neat PVA). PVA chain movements could be restricted, leading this results, due to the formation of PVA-PAA hydrogen bonds (as were inferred from FTIR results) (Chen and Zhang 2010).

The magnetic properties of the prepared MNPs were reported in detail in a previous work (Sanchez et al. 2018a). Regarding the magnetic properties of the ferrogel samples, results are summarized in Table 4. Curves for magnetization vs. field obtained from VSM measurements are shown in Fig. 9 for the PAA Mw = 5000 ferrogels.

As can be seen, the higher the MNP content, higher saturation magnetization (Ms) and susceptibility (χ) for both kinds of ferrogels. Furthermore, for similar MNP contents, Ms and χ are higher when PAA Mw 5000 is employed. In general, all ferrogels showed an increase in their Ms when MNPs content increases: this fact could be related to an agglomeration effect.

Pollutant adsorption experiments

The effectiveness of developed materials to remove different contaminants was evaluated. Figure 10 includes the removal of MB by the PVA hydrogel and several ferrogels, with and without the application of an external magnetic field through the employment of equipment specially developed to this (Fig. 11).

It is possible to observe that, after 360 min, maximum MB removal levels near to 55–65% were achieved by PVA hydrogel and also by some of the ferrogels with the minor contents of MNPs. Although the tendencies found are varied, the tests conducted by applying an external magnetic field shown little removal differences at high MNPs contents when they are compared with the analogous system without it during the first hours of treatment.

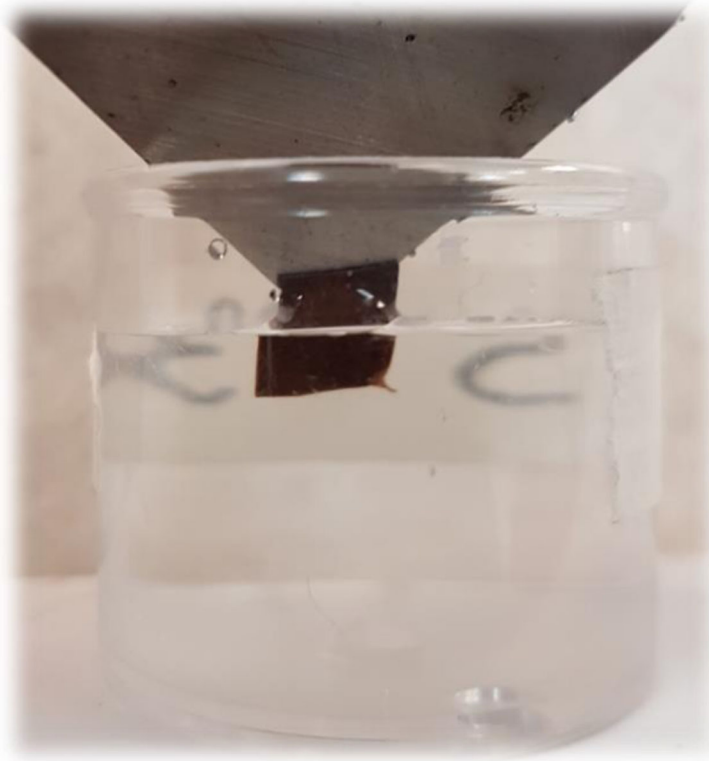

Fig. 12 Ferrogel removal after the corresponding water treatment

After 2 days, ferrogels with low MNPs contents have shown removal level upper to 70%, more than that achieved by the neat hydrogel. In all cases, the advantages of having MNPs for the simple gel removal after the corresponding water treatment should be considered (Fig. 12).

In order to find out the kinetic model that better fits to the adsorption process, two kinetic models were applied (Liu et al. 2010). The first one was the pseudo first-order kinetic model of Lagergren (Eq. 7):

$$\log(q_{1e}-q_t) = logq_{1e} - \frac{K_1\ t}{2.303} \tag{7}$$

where q_{1e} and q_t represent the amount of dye adsorbed on the adsorbent at equilibrium and at any time, respectively, and K_1 (min^{-1}) is the rate constant.

Table 5 Kinetic parameters of the two models applied for MB adsorption onto the ferrogel

Adsorbent		Pseudo first-order			q_{exp} (mg/g)	Pseudo second-order		
		K_1 (min^{-1})	R^2	q_{1e} (mg/g)		q_{2e} (mg/g)	R^2	K_2 (g/(mg min))
PVA		0.0009	0.6553	5.028	1.426	1.449	0.9999	0.0178
PVA/PAA Mw 1800	2.2% MNPs mf*	0.0032	0.8648	4.334	0.773	0.819	0.9982	0.0074
	2.2% MNPs	0.0029	0.9444	4.016	0.691	0.744	0.9978	0.0065
	5.8% MNPs mf*	0.0032	0.9650	9.521	1.103	1.232	0.9976	0.0023
	5.8% MNPs	0.0037	0.9980	10.990	1.156	1.307	0.9995	0.0020
PVA/PAA Mw 5000	2.3% MNPs mf*	0.0032	0.8696	6.869	1.625	1.673	0.9998	0.0137
	2.3% MNPs	0.0009	0.9539	2.203	1.565	1.583	0.9998	0.0174
	11.2% MNPs mf*	0.0029	0.9500	5.373	0.891	0.917	0.9996	0.0055
	11.2% MNPs	0.0041	0.9520	15.592	1.336	1.396	0.9984	0.0022

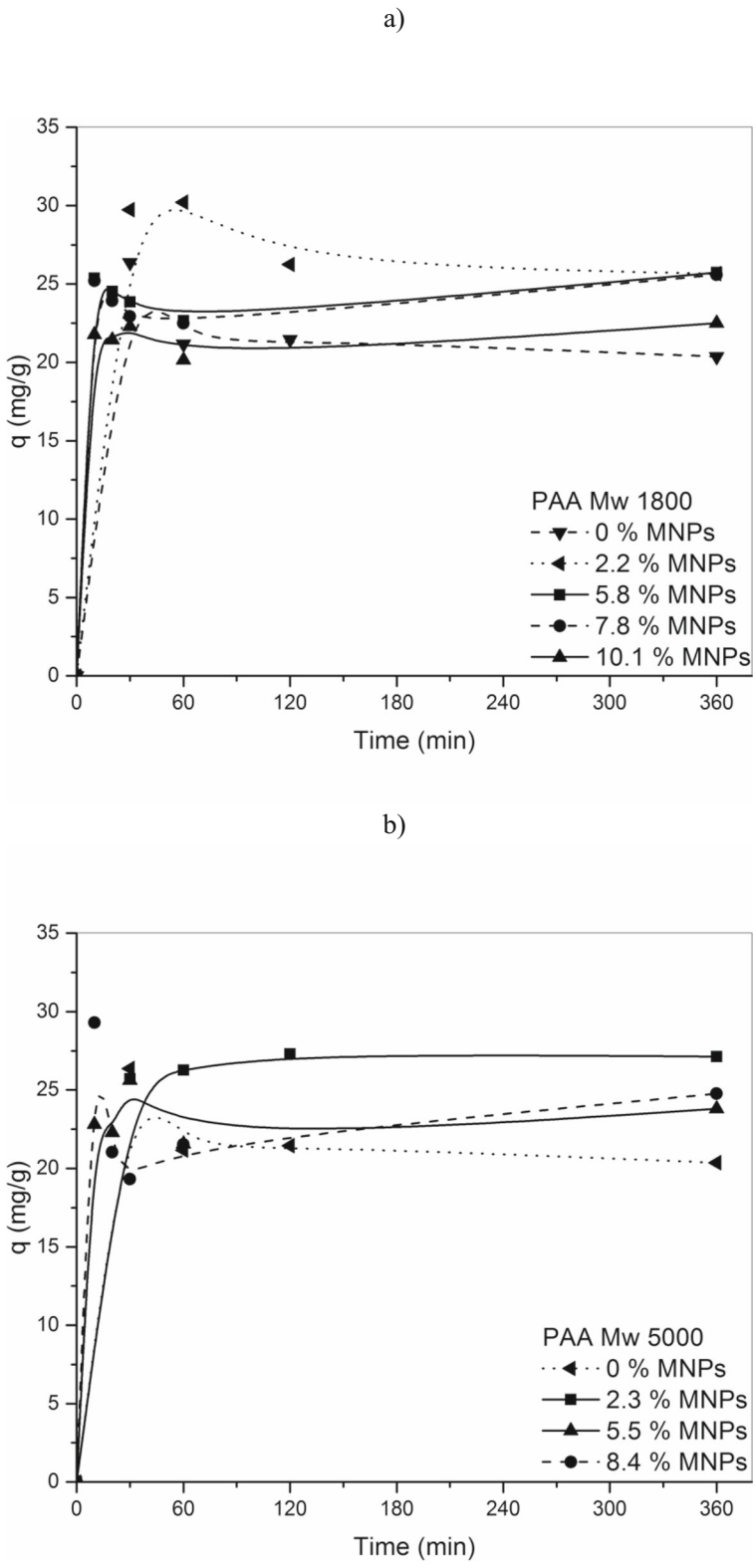

Fig. 13 Adsorption of Cd^{+2} by PVA hydrogel and ferrogels with several amounts of MNPs coated with PAA of different Mw 1800 (a) and 5000 (b)

Table 6 Kinetic parameters of the pseudo second-order kinetic model applied for Cd^{+2} adsorption onto the ferrogel

Adsorbent		q_{exp} (mg/g)	Pseudo second-order		
			q_{2e} (mg/g)	R^2	K_2 (g/(mg min))
PVA		20.36	20.04	0.9998	0.0083
PVA/PAA Mw 1800	2.2% MNPs	25.66	25.18	0.9997	0.0016
	5.8% MNPs	25.72	25.91	0.9995	0.0132
	7.8% MNPs	25.59	25.77	0.9995	0.0115
	10.1% MNPs	22.50	22.57	0.9996	0.0208
PVA/PAA Mw 5000	2.3% MNPs	27.31	27.47	1.000	0.0169
	5.5% MNPs	23.80	23.87	0.9996	0.0256
	8.4% MNPs	24.76	25.06	0.9991	0.0079

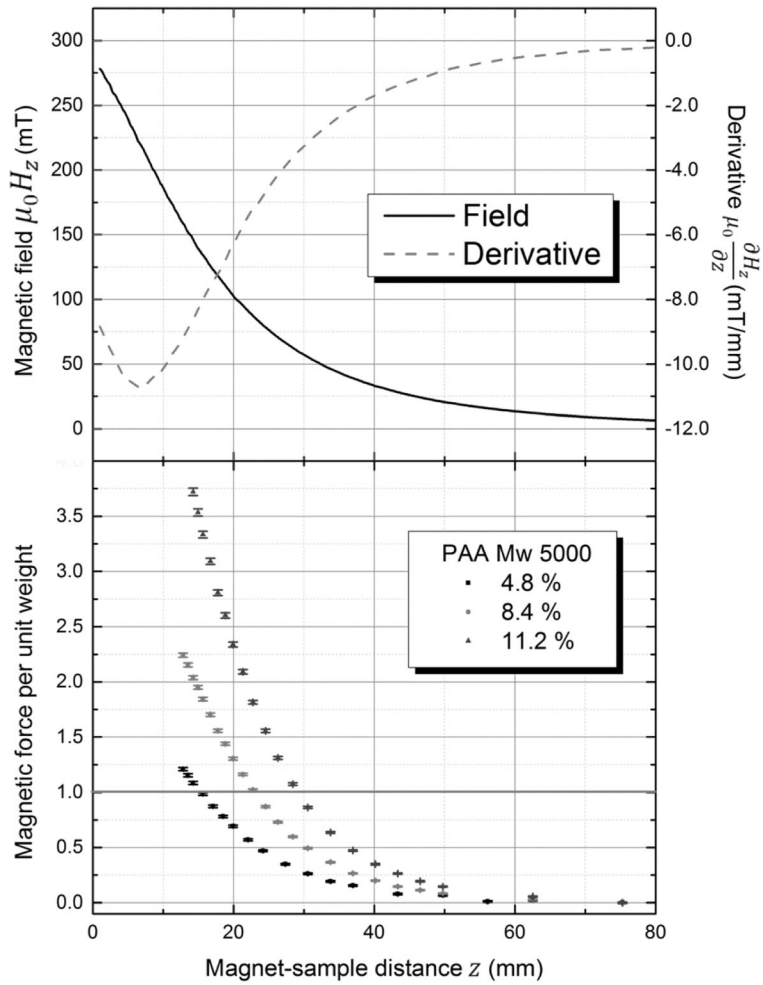

Fig. 14 Vertical component of the magnetic field and its derivative with respect to the magnet-sample distance z, both on the magnet's axis and as functions of z (top). Magnetic force per unit weight (dimensionless) vs. z, for the three ferrogels with MNPs coated with PAA of Mw 5000 (bottom). The magenta line represents the threshold over which the sample would be lifted by the magnet

On the other side, the linear form of Ho's pseudo second-order kinetics is shown in Eq. 8:

$$\frac{t}{q_t} = \frac{1}{\left(K_2\, q_{2e}^2\right)} + \frac{t}{q_{2e}} \tag{8}$$

where q_{2e} and q_t represent the same as above-described, respectively, and K_2 (g/mg min) is the corresponding rate constant.

The obtained results are summarized in Table 5.

The model that better fits is the pseudo second-order one since the correlation coefficient (R^2) is close to 1.0. Additionally, it can be observed that q_{2e} values obtained by fitting are closer to the experimental values (q_{exp}) than to q_{1e} ones.

Finally, the removal of Cd^{+2} from aqueous model solutions was also tested. Fig. 13 displayed the obtained results. As can be seen, the different ferrogels offer better results for Cd^{+2} removal than neat PVA matrix. The general trend in terms of MNPs content and removal capability is similar to the observed in MB tests: the smaller MNPs amount the higher removal is achieved.

Pseudo first- and second-order kinetic models were also employed to understand the Cd^{+2} adsorption process. Once again, the best-fit model was the second one and the corresponding results are summarized in Table 6.

Magnetic force experiments

For the ferrogels with MNPs coated with PAA of Mw 5000, samples of 1.5 cm × 1.5 cm were placed on the base on the balance. The magnetic force was measured as a function of the distance to the magnet pole surface, starting high above enough so that the force was zero and then lowering the magnet.

Equation 6 shows the dependence of this force with the sample's magnetization (which is in turn a function of the field) and the field's derivative. Both the field generated by the $Nd_2Fe_{14}B$ magnet and its derivative are shown in Fig. 14a as function of the distance between the sample and the magnet's surface. Figure 14b shows the results for the magnetic force measurements, where the magenta line represents the force per unit weight threshold; any value above unity is enough to lift the sample. As expected, the force per unit weight increases with MNPs' concentration. These results show promise for the recovery of the ferrogel after adsorption.

Conclusions

In this work, several ferrogels were prepared in our laboratory by a simple and non-toxic technique, and they were also fully characterized. It was found that the incorporation of PAA-magnetic nanoparticles on the PVA matrix produced a set of changes: increases on the thermal resistance, changes on the swelling behavior, and variations on the morphology regarding the neat hydrogel. All these results were attributed to the interactions between the matrix and the MNPs (mainly studied by FTIR).

Ferrogels captured in an efficient mode common toxic residues (Cd^{+2} and MB) from water and after this they were effectively magnetically separated. Moreover, it was checked that the polymer architecture and the polymer matrix present in the gel used for this application complies with the requirement of being light enough, even when it is completely swollen, to allow the forces created by the magnetic particles being able to capture the gel with a permanent magnet.

All results give the idea that the developed material could be a potential solution for water decontamination.

Acknowledgements The authors acknowledge the collaborations made by Dra. Romina P. Ollier and Dra. M. Fernanda Horst.

Funding information This study received funding from CONICET (PIP00617), Universidad Nacional de Mar del Plata, Universidad Nacional de La Plata (X807), ANPCyT (PICT 2014-3228 and PICT 2016-1905) and Fundación Bunge & Born.

Compliance with ethical standards

Conflict of interest The authors declare that they have no conflict of interest.

References

Ahmed EM (2015) Hydrogel: preparation, characterization, and applications: a review. J Adv Res 6:105–121. https://doi.org/10.1016/j.jare.2013.07.006

Alghanmi S, Al Sulami A, El-Zayat T et al (2015) Acid leaching of heavy metals from contaminated soil collected from Jeddaj, Saudi Arabia: kinetic and thermodynamics studies. Int Soil Water Conserv Res 3:196–208

Bardajee GR, Hooshyar Z, Rastgo F (2013) Kappa carrageenan-g-poly (acrylic acid)/SPION nanocomposite as a novel stimuli-sensitive drug delivery system. Colloid Polym Sci 291:2791–2803. https://doi.org/10.1007/s00396-013-3018-6

Bonhome Espinosa AB (2017) Hidrogeles magnéticos para aplicaciones biomédicas. Estudio de su biocompatibilidad y propiedades viscoelásticas Universidad de Granada (España)

Byun H, Hong B, Nam SY, Jung SY, Rhim JW, Lee SB, Moon GY (2008) Swelling behavior and drug release of poly (vinyl alcohol) hydrogel cross-linked with poly (acrylic acid). Macromol Res 16:189–193

Chen NX, Zhang JH (2010) The role of hydrogen-bonding interaction in poly(vinyl alcohol)/ poly(acrylic acid) blending solutions and their films. Chinese J Polym Sci (Eng Ed) 28: 903–911. https://doi.org/10.1007/s10118-010-9167-x

Goiti E, Salinas MM, Arias G, Puglia D, Kenny JM, Mijangos C (2007) Effect of magnetic nanoparticles on the thermal properties of some hydrogels. Polym Degrad Stab 92:2198–2205. https://doi.org/10.1016/j.polymdegradstab.2007.02.025

Gonzalez JS, Alvarez VA (2011) The effect of the annealing on the poly(vinyl alcohol) obtained by freezing-thawing. Thermochim Acta 521:184–190. https://doi.org/10.1016/j.tca.2011.04.022

Gonzalez JS, Nicolás P, Ferreira ML, Avena M, Lassalle VL, Alvarez VA (2014) Fabrication of ferrogels using different magnetic nanoparticles and their performance on protein adsorption. Polym Int 63:258–265. https://doi.org/10.1002/pi.4498

Gonzalez J, Ponce A, Alvarez V (2016) Preparation and characterization of poly (vinylalcohol) / bentonite hydrogels for potential wound dressings. Adv Mater Lett 7:979–985. https://doi.org/10.5185/amlett.2016.6888

Gudman L, Peppas NA (1995) Preparation and characterization of pH-sensitive , interpenetrating networks of poly (vinyl alcohol) and poly (acrylic acid). J Appl Polym Sci 55:919–928. https://doi.org/10.1002/app.1995.070550610

Gupta S, Pramanik AK, Kailath A, Mishra T, Guha A, Nayar S, Sinha A (2009) Composition dependent structural modulations in transparent poly(vinyl alcohol) hydrogels. Colloids Surf B Biointerfaces 74:186–190. https://doi.org/10.1016/j.colsurfb.2009.07.015

Hickey AS, Peppas NA (1997) Solute diffusion in poly(vinyl alcohol)/poly(acrylic acid) composite membranes prepared by freezing/thawing techniques. Polymer (Guildf) 38:5931–5936. https://doi.org/10.1016/S0032-3861(97)00163-8

Kim JI, Chun C, Kim B, Hong JM, Cho JK, Lee SH, Song SC (2012) Thermosensitive/magnetic poly(organophosphazene) hydrogel as a long-term magnetic resonance contrast platform. Biomaterials 33:218–224. https://doi.org/10.1016/j.biomaterials.2011.09.033

Kumar M, Tamilarasan R (2013) Modeling studies: adsorption of aniline blue by using Prosopis Juliflora carbon/Ca/alginate polymer composite beads. Carbohydr Polym 92:2171–2180. https://doi.org/10.1016/j.carbpol.2012.11.076

Lin CL, Lee CF, Chiu WY (2005) Preparation and properties of poly(acrylic acid) oligomer stabilized superparamagnetic ferrofluid. J Colloid Interface Sci 291:411–420. https://doi.org/10.1016/j.jcis.2005.05.023

Liu Y, Zheng Y, Wang A (2010) Enhanced adsorption of methylene blue from aqueous solution by chitosan-g-poly (acrylic acid)/vermiculite hydrogel composites. J Environ Sci 22: 486–493. https://doi.org/10.1016/S1001-0742(10)60438-X

Majid S, Bukhari H, Khan S et al (2015) Synthesis and characterization of chemically cross-linked acrylic acid / gelatin hydrogels : effect of pH and composition on swelling and drug release. Int J Polym Sci 15

Manavi-Tehrani I, Rabiee M, Parviz M, Tahriri MR, Fahimi Z (2010) Preparation, characterization and controlled release investigation of biocompatible pH-sensitive PVA/PAA hydrogels. Macromol Symp 296:457–465. https://doi.org/10.1002/masy.201051062

Mansur HS, Oréfice RL, Mansur AAP (2004) Characterization of poly(vinyl alcohol)/poly(ethylene glycol) hydrogels and PVA-derived hybrids by small-angle X-ray scattering and FTIR spectroscopy. Polymer (Guildf) 45:7193–7202. https://doi.org/10.1016/j.polymer.2004.08.036

Mansur HS, Sadahira CM, Souza AN, Mansur AAP (2008) FTIR spectroscopy characterization of poly (vinyl alcohol) hydrogel with different hydrolysis degree and chemically crosslinked with glutaraldehyde. Mater Sci Eng C 28:539–548. https://doi.org/10.1016/j.msec.2007.10.088

Mendoza Zelis P, Muraca D, Gonzalez JS et al (2013) Magnetic properties study of iron-oxide nanoparticles/PVA ferrogels with potential biomedical applications. J Nanopart Res 15: 1613. https://doi.org/10.1007/s11051-013-1613-6

Moscoso-Londono O, Muraca D, de Oliveira L et al (2013) The effect of coated-Fe3O4 nanoparticles on magnetic properties of ferrogels produced by diffusion route. IEEE Trans Magn 49: 4551–4554. https://doi.org/10.1109/TMAG.2013.2259804

Nigam P, Armour G, Banat IM, Singh D, Marchant R (2000) Physical removal of textile dyes from effluents and solid-state fermentation of dye-adsorbed agricultural residues. Bioresour Technol 72:219–226. https://doi.org/10.1016/S0960-8524(99)00123-6

Peppas NA, Tennenhouse D (2004) Semicrystalline poly (vinyl alcohol) films and their blends with poly (acrylic acid) and poly (ethylene glycol) for drug delivery applications. J Drug Del Sci Technol 14:291–297

Peppas NA, Wright SL (1998) Drug diffusion and binding in ionizable interpenetrating networks from poly(vinyl alcohol) and poly(acrylic acid). Eur J Pharm Biopharm 46:15–29. https://doi.org/10.1016/S0939-6411(97)00113-6

Quintero SMM, Ponce FRV, Cremona M et al (2010) Swelling and morphological properties of poly(vinyl alcohol) (PVA) and poly(acrylic acid) (PAA) hydrogels in solution with high salt concentration. Polymer (Guildf) 51:953–958. https://doi.org/10.1016/j.polymer.2009.12.016

Ray D, Mohanta GP, Gils PS et al (2009) Delivery of antihypertensive drug through synthesized hydrogel network, a comparative study. Lat Am J Pharm 28:747–755

Reddy DHK, Lee SM (2013) Application of magnetic chitosan composites for the removal of toxic metal and dyes from aqueous solutions. Adv Colloid Interf Sci 201–202:68–93. https://doi.org/10.1016/j.cis.2013.10.002

Ricciardi R, Auriemma F, Gaillet C, de Rosa C, Lauprêtre F (2004) Investigation of the crystallinity of freeze/thaw poly(vinyl alcohol) hydrogels by different techniques. Macromolecules 37:9510–9516. https://doi.org/10.1021/ma048418v

Sanchez LM, Alvarez VA, Gonzalez JS (2016) Ferrogels: smart materials for biomedical and remediation applications. In: Handbook of composites from renewable materials, volume 8: nanocomposites: advanced applications. pp 400–430

Sanchez LM, Alvarez VA, Gonzalez JS (2017) 21. Ferrogels : smart materials for biomedical and remediation applications. In: Handbook of composites from renewable materials

Sanchez LM, Martin DA, Alvarez VA, Gonzalez JS (2018a) Polyacrylic acid-coated iron oxide magnetic nanoparticles: the polymer molecular weight influence. Colloids Surf A

Physicochem Eng Asp 543. https://doi.org/10.1016/j.colsurfa.2018.01.050

Sanchez LM, Ollier RP, Gonzalez JS, Alvarez VA (2018b) Chapter 51. Nanocomposite materials for dyes removal. In: Handbook of nanomaterials for industrial applications. p 1143

Sekhavat Pour Z, Ghaemy M (2015) Removal of dyes and heavy metal ions from water by magnetic hydrogel beads based on poly(vinyl alcohol)/carboxymethyl starch-g-poly(vinyl imidazole). RSC Adv 5:64106–64118. https://doi.org/10.1039/C5RA08025H

Sinha Ray S, Okamoto M (2003) Polymer/layered silicate nanocomposites: a review from preparation to processing. Prog Polym Sci 28:1539–1641. https://doi.org/10.1016/j.progpolymsci.2003.08.002

Smith TJ, Kennedy JE, Higginbotham CL (2009) Development of a novel porous cryo-foam for potential wound healing applications. J Mater Sci Mater Med 20:1193–1199. https://doi.org/10.1007/s10856-008-3670-4

Sorber J, Steiner G, Schulz V, Guenther M, Gerlach G, Salzer R, Arndt KF (2008) Hydrogel-based piezoresistive pH sensors: investigations using FT-IR attenuated total reflection spectroscopic imaging. Anal Chem 80:2957–2962. https://doi.org/10.1021/ac702598n

Sun Y, Zhang Z, Moon KS, Wong CP (2004) Glass transition and relaxation behavior of epoxy nanocomposites. J Polym Sci Part B Polym Phys 42:3849–3858. https://doi.org/10.1002/polb.20251

Sun X-F, Baichen L, Jing Z, Wang H (2015) Preparation and adsorption property of xylan/poly(acrylic acid) magnetic nanocomposite hydrogel adsorbent. Carbohydr Polym 118:16–23. https://doi.org/10.1016/j.carbpol.2014.11.013

Timko BP, Dvir T, Kohane DS (2010) Remotely triggerable drug delivery systems. Adv Mater 22:4925–4943. https://doi.org/10.1002/adma.201002072

Vazquez Torres H, Cauich Rosriguez J, Cruz Ramos C (1993) Poly (vinyl alcohol)/ poly (acrylic acid) blends : miscibility studies by DSC and characterization of their thermally induced hydrogels. J Appl Polym Sci 50:777–792